




Article

Direct Rehydrogenation of LiBH_4 from H-Deficient $\text{Li}_2\text{B}_{12}\text{H}_{12-x}$

Yigang Yan ¹, Hui Wang ², Min Zhu ², Weitong Cai ³ , Daniel Rentsch ⁴  and Arndt Remhof ^{4,*} 

¹ Center for Materials Crystallography (CMC), the Department of Chemistry and the Interdisciplinary Nanoscience Center (iNANO), Aarhus University, Langelandsgade 140, 8000 Aarhus, Denmark; yigang.yan@inano.au.dk

² School of Materials Science and Engineering, Guangdong Provincial Key Laboratory of Advanced Energy Storage Materials, South China University of Technology, Guangzhou 510640, China; mehawang@scut.edu.cn (H.W.); memzhu@scut.edu.cn (M.Z.)

³ School of Materials and Energy, Guangdong University of Technology, Guangzhou 510006, China; mewtcai@gdut.edu.cn

⁴ Empa-Swiss Federal Laboratories for Materials Science and Technology, 8600 Dübendorf, Switzerland; Daniel.Rentsch@empa.ch

* Correspondence: arndt.remhof@empa.ch

Received: 22 January 2018; Accepted: 6 March 2018; Published: 9 March 2018

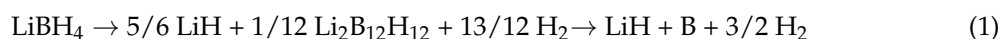
Abstract: $\text{Li}_2\text{B}_{12}\text{H}_{12}$ is commonly considered as a boron sink hindering the reversible hydrogen sorption of LiBH_4 . Recently, in the dehydrogenation process of LiBH_4 an amorphous H-deficient $\text{Li}_2\text{B}_{12}\text{H}_{12-x}$ phase was observed. In the present study, we investigate the rehydrogenation properties of $\text{Li}_2\text{B}_{12}\text{H}_{12-x}$ to form LiBH_4 . With addition of nanostructured cobalt boride in a 1:1 mass ratio, the rehydrogenation properties of $\text{Li}_2\text{B}_{12}\text{H}_{12-x}$ are improved, where LiBH_4 forms under milder conditions (e.g., 400 °C, 100 bar H_2) with a yield of 68%. The active catalytic species in the reversible sorption reaction is suggested to be nonmetallic Co_xB ($x = 1$) based on ^{11}B MAS NMR experiments and its role has been discussed.

Keywords: hydrogen storage; lithium borohydride; nuclear magnetic resonance

1. Introduction

Hydrogen is considered to be an ideal synthetic energy carrier to replace the limited quantity of fossil fuels available. Wide utilization of hydrogen as a fuel source for mobile applications requires the storage material to be safe, efficiently store hydrogen, and transportable. Owing to high gravimetric and volumetric densities of hydrogen, metal borohydrides have been intensively investigated for solid-state hydrogen storage over the last decade [1–6]. Among them, lithium borohydride (LiBH_4), exhibiting a hydrogen density of 18.5 wt %, is one of the currently most discussed lightweight complex hydrides [7–18]. It crystallizes in two polymorphs, with structural transition from an orthorhombic low-temperature phase to a hexagonal high-temperature (HT) phase above 110 °C [7].

LiBH_4 melts at $T_m = 280$ °C and releases considerable amounts of hydrogen from the liquid state. The decomposition pathway of LiBH_4 depends on temperature and H_2 pressure with $\text{Li}_2\text{B}_{12}\text{H}_{12}$ formed as the main intermediate compound following a two-step route [10,13]:



Experimentally, a H-deficient $\text{Li}_2\text{B}_{12}\text{H}_{12-x}$ phase has been identified in the solid residue of the thermal decomposition of LiBH_4 [13,14]. $\text{Li}_2\text{B}_{12}\text{H}_{12-x}$ further decomposes into elemental boron above

650 °C [14]. Owing to the high thermal stability and low chemical reactivity, $\text{Li}_2\text{B}_{12}\text{H}_{12}$ is generally considered as a boron sink in the hydrogen sorption process of LiBH_4 -based compounds hindering the efficient rehydrogenation reaction. Many efforts have been taken to circumvent the formation of $\text{Li}_2\text{B}_{12}\text{H}_{12}$ in dehydrogenation process of LiBH_4 and to improve the reversibility [18–29]. However, much less work has been done on the hydrogenation properties of $\text{Li}_2\text{B}_{12}\text{H}_{12}$ itself, especially of the H-deficient $\text{Li}_2\text{B}_{12}\text{H}_{12-x}$ formed from the decomposition of LiBH_4 , which is of great importance for improving the hydrogen storage function of LiBH_4 .

The reformation of LiBH_4 from its decomposition products was observed at 600 °C under a H_2 pressure of 150 to 350 bar [9,11]. However, due to the amorphous state of the boron-containing compound in the decomposition product, the reaction pathway of the reformation of LiBH_4 is not well documented. Recently, the reactivity of crystalline $\text{Li}_2\text{B}_{12}\text{H}_{12}$ and LiH with a molar ratio of 1 to 10 has been examined, which convert to LiBH_4 at 500 °C within 72 h. However, a high H_2 pressure of 1000 bar is required to overcome the high kinetic barrier in the hydrogenation reaction [17].

In the present study, we systematically investigated the rehydrogenation properties of $\text{Li}_2\text{B}_{12}\text{H}_{12-x}$ to form LiBH_4 . First, pure LiBH_4 was decomposed to $\text{Li}_2\text{B}_{12}\text{H}_{12-x}$ at 600 °C. The rehydrogenation of the $\text{Li}_2\text{B}_{12}\text{H}_{12-x}$ was carried out under the conditions of 350 bar H_2 , 500 to 600 °C and 24 h. Second, nanostructured cobalt boride was added to LiBH_4 in a weight ratio of 1:1, enabling the decomposition of LiBH_4 to $\text{Li}_2\text{B}_{12}\text{H}_{12-x}$ already at 350 °C. In presence of cobalt boride, the rehydrogenation of $\text{Li}_2\text{B}_{12}\text{H}_{12-x}$ is facilitated, where the reformation of LiBH_4 is achieved under relatively mild conditions (e.g., 400 °C and 100 bar H_2). We investigated the active catalytic species of cobalt boride and discuss the catalytic mechanism.

2. Experimental

The starting material, LiBH_4 (purity, 95%) was purchased from Sigma-Aldrich Corp (St. Louis, MO, USA). Waxberry-like nanostructured cobalt boride was synthesized based on a wet-chemistry method described in literature [15,30,31]. The nanostructured cobalt boride shows a specific surface area of 39.7 m^2/g and approximate average composition of $\text{Co}_{1.34}\text{B}$ [15]. The as-synthesized $\text{Co}_{1.34}\text{B}$ and LiBH_4 were mechanically milled in a weight ratio of 1:1 using vibration milling (QM-3C, Nanjing Nanda Instrument Plant, Nanjing, China) for 1 h with a ball to powder ratio of 120:1 under Ar atmosphere. In the as-prepared sample 80.5 mol % of the boron originate from LiBH_4 , the remaining 19.5 mol % from $\text{Co}_{1.34}\text{B}$. The H_2 desorption of the as-prepared $\text{LiBH}_4\text{-Co}_{1.34}\text{B}$ composite was performed using a custom-made pressure-composition-temperature apparatus under dynamic vacuum (lower than 10^{-4} mbar). The hydrogen amount was determined by the gas flow by means of a flow meter.

Solid state ^{11}B magic angle spinning (MAS) NMR experiments were performed on a Bruker Avance-400 NMR spectrometer (Bruker BioSpin AG, Fällanden, Switzerland) using a 4 mm CP-MAS probe. The ^{11}B MAS NMR spectra were recorded at 128.4 MHz at 12 kHz sample rotation applying a Hahn echo pulse sequence to suppress the broad background resonance of boron nitride in the probe. Pulse lengths of 1.5 μs ($\pi/12$ pulse) and 3.0 μs were applied for the excitation and echo pulses, respectively. For selected samples, ^1H - ^{11}B -cross polarization magic angle spinning (CP-MAS) NMR experiments were performed using weak radio-frequency powers for spin locking of the ^{11}B nucleus on resonance with mixing times of 50 μs . The setup was performed using LiBH_4 , for a sample of $\text{B}(\text{OH})_3$ only a very weak CP transfer efficiency was observed (<2% of signal intensity compared to a single pulse experiment). ^{11}B NMR chemical shifts are reported in parts per million (ppm) externally referenced to a 1 M $\text{B}(\text{OH})_3$ aqueous solution at 19.6 ppm as external standard sample. Quadrupolar parameters of B(III) sites and relative amounts of three- and four-fold coordinated boron atoms were determined by non-linear least-square fits of the regions of interest using the software DMFIT [32].

3. Results

To improve the reversibility the de- and rehydrogenation reaction of LiBH_4 , 50 wt % waxberry-like nanostructured Co_xB ($x = 1.34$) was introduced into LiBH_4 by ball milling. In the past, different

$\text{Co}_x\text{B}:\text{LiBH}_4$ ratios were investigated. The 1:1 ratio showed the optimal hydrogen sorption performance [15]. The present study is to further investigate the hydrogen sorption mechanism of the $\text{Co}_x\text{B}:\text{LiBH}_4$ composite. Therefore, only the 1:1 ratio sample is investigated here. Figure 1a depicts the hydrogen desorption profile up to 500 °C. The $\text{LiBH}_4\text{-Co}_{1.34}\text{B}$ composite shows two hydrogen desorption events at 200 and 375 °C, respectively, which are in agreement with previously reported results [15]. The major hydrogen desorption occurs around 375 °C. Figure 1b shows the isothermal dehydrogenation at 350 °C in the first two cycles. The rehydrogenation was carried out at 400 °C and 100 bar H_2 for 24 h after the first dehydrogenation. The composite releases 5.1 wt % and 3.6 wt % hydrogen in the first two cycles, respectively, indicating a reversibility of 68%.

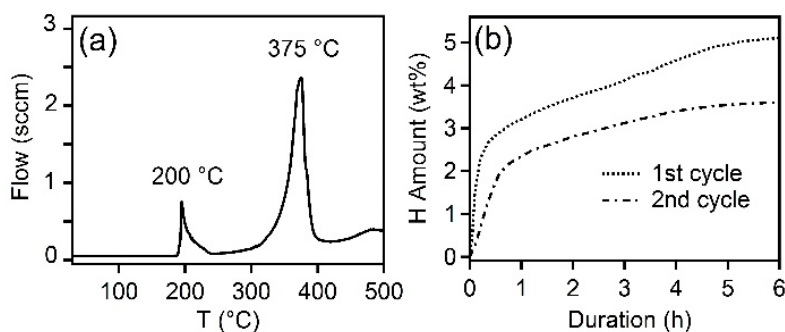


Figure 1. (a) Hydrogen desorption profile up to 500 °C; (b) isothermal hydrogen release of $\text{LiBH}_4\text{-Co}_{1.34}\text{B}$ at 350 °C in the first two cycles.

Figure 2a shows the full-range ^{11}B MAS NMR spectra of the $\text{LiBH}_4\text{-Co}_{1.34}\text{B}$ composite at different reaction states, compared to LiBH_4 . The center band in the ^{11}B NMR spectrum in the as-prepared composite is observed at -41.9 ppm corresponding to the resonance of LiBH_4 . The signal maximum shifts to -10.3 ppm after dehydrogenation indicating the formation of intermediate products and returns to -41.9 ppm after rehydrogenation confirming that a large portion of LiBH_4 has been reformed. Note that the as-prepared $\text{LiBH}_4\text{-Co}_{1.34}\text{B}$ composite shows very strong sidebands in the ^{11}B MAS NMR spectrum, while the side bands are much weaker in the spectra of the other samples shown in Figure 2a. We attribute the intense spinning side bands over a large chemical shift range in the as-prepared sample to the presence of ferromagnetism in the initial $\text{Co}_{1.34}\text{B}$, as discussed in more detail below.

Figure 2b,c compare the central parts of the ^{11}B MAS and the $^1\text{H}\text{-}^{11}\text{B}$ CP-MAS NMR spectra of the products after dehydrogenation at 350 °C and rehydrogenation at 400 °C. In Figure 2b the observed center band resonance can be deconvoluted into a main resonance at -10.3 ppm, and minor resonances at -41.0 , 5.3 and 17.0 ppm. The resonances at -10.3 ppm and at -41.0 ppm are assignable to $\text{Li}_2\text{B}_{12}\text{H}_{12-x}$ and LiBH_4 , respectively. In the $^1\text{H}\text{-}^{11}\text{B}$ CP-MAS NMR spectra both signals still are present, whereas all other resonances belong to boron containing chemical species not attached to protons. The resonances at 5.3 and 17.0 ppm showing a typical second-order quadrupole pattern represent about 19 mol % of the boron atoms in the dehydrogenated state (Figure 2b), corresponding to the initial $\text{LiBH}_4:\text{Co}_x\text{B}$ ratio. Therefore, these resonances are tentatively attributed to Co_xB . On the other hand, the shape of these resonances resembles the one of the line shape of $\text{B}(\text{OH})_3$ [33]. However, the evaluated quadrupolar coupling constant and the chemical shift are slightly different and a strong contamination with oxygen is unlikely. In Figure 2c the main signal at -41 ppm is assigned to LiBH_4 and a minor resonance at -15.5 ppm originates from stoichiometric $\text{Li}_2\text{B}_{12}\text{H}_{12}$. An unambiguous quantification of Co_xB by NMR is hampered by the presence of magnetic and chemical impurities.

Previous XRD studies indicate the formation of a new compound i.e., Co_xB ($x = 1$) [15]. In the present experiment we see a strong decrease of the ferromagnetic signal by the reduced intensity of the spinning side bands in the ^{11}B MAS NMR spectra upon the first hydrogen cycling. This is an indirect

evidence of the formation of Co_xB ($x = 1$). The magnetism of Co_xB is known to decrease with increasing boron concentration, i.e., Co_3B and Co_2B are ferromagnetic while CoB is non-magnetic [34,35].

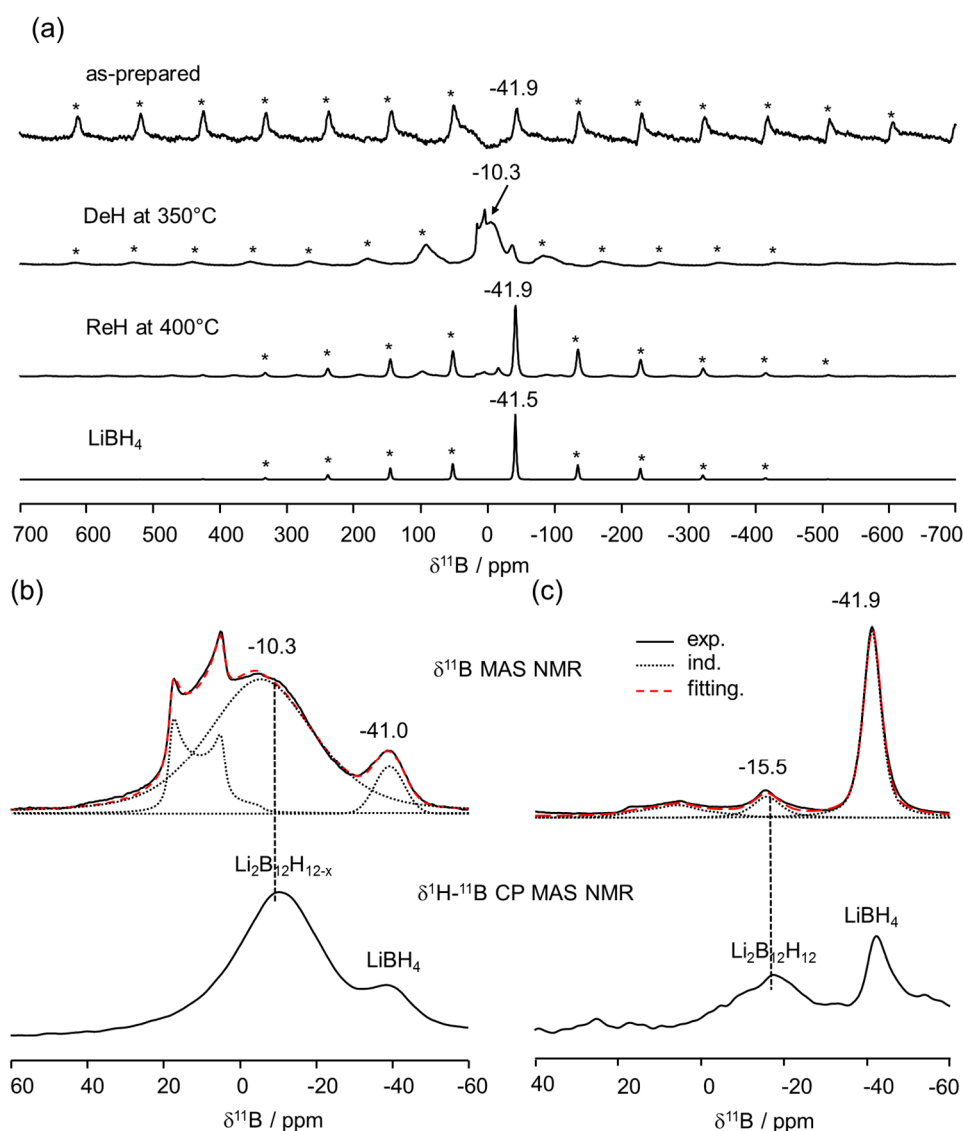


Figure 2. (a) Full range of ^{11}B MAS NMR spectra of $\text{LiBH}_4\text{-Co}_{0.34}\text{B}$ composite at different reaction stages: as-prepared, dehydrogenated (DeH) at 350 °C, rehydrogenated (ReH) at 400 °C, and of pure LiBH_4 as reference; (b,c) ^{11}B MAS NMR and ^1H - ^{11}B CP-MAS NMR spectra of the $\text{LiBH}_4\text{-Co}_{0.34}\text{B}$ composite dehydrogenated at 350 °C and rehydrogenated at 400 °C, respectively. The experimental data (exp.) are shown as solid, individual components (ind.) and fitting results as different dotted (···) and broken (---) lines, respectively. The stars (*) indicate spinning side bands.

4. Discussion

The direct rehydrogenation of LiBH_4 from its decomposition products only occurs at harsh conditions, e.g., 600 °C under 155 bar H_2 [11]. We significantly improve the rehydrogenation properties of LiBH_4 from its decomposition products $\text{Li}_2\text{B}_{12}\text{H}_{12-x}$ and LiH by addition of nanocrystalline cobalt boride ($\text{Co}_{0.34}\text{B}$), the rehydrogenation of LiBH_4 from its decomposition product $\text{Li}_2\text{B}_{12}\text{H}_{12-x}$ and LiH occurs already at much lower temperature (400 °C) and pressure (100 bar H_2) with a yield of 68%. In addition, under catalysis of cobalt boride, the dehydrogenation reaction of LiBH_4 to $\text{Li}_2\text{B}_{12}\text{H}_{12-x}$ is feasible at a lower temperature, i.e., 350 °C. The chemical state of cobalt changed

during the hydrogen sorption process from the Co-rich, ferromagnetic $\text{Co}_{1.34}\text{B}$ to the non-magnetic Co_xB ($x = 1$).

The catalytic effect of cobalt borides has been reported in other hydrogen-related reactions [36–38]. For instance, metallic Co and metallic-like Co_2B were reported to decrease remarkably the dehydrogenation temperature in the $\text{LiBH}_4/\text{LiNH}_2$ system [36]. Nanocrystalline Co_2B was also found to act as an efficient catalyst for hydrogen production from the hydrolysis of NaBH_4 and in the field of electrochemical water splitting [36,38]. This is different from the result in the present study, where ^{11}B MAS NMR results suggest that the active catalytic species must be nonmetallic and nonmagnetic with a composition close to CoB (1:1 in molar ratio). The catalytic effect of cobalt borides could be attributed to their non-compensated electronic structure, where electron transfers from B to a vacant d-orbital of metallic Co, making B electron-deficient and Co electron-enriched [39,40]. Thereby cobalt borides may be able to promote the formation of B-H bonds of $[\text{BH}_4]^-$ during dehydrogenation and enable the break of B-H bonds in $\text{Li}_2\text{B}_{12}\text{H}_{12-x}$ in the rehydrogenation process. In the present case, the formation of Co_xB ($x = 1$) from $\text{Co}_{1.34}\text{B}$ requires the addition of boron, which may originate from $\text{Li}_2\text{B}_{12}\text{H}_{12-x}$, leading to a partial decomposition of the stable B_{12} units. In this scenario, cobalt boride would act as an additive rather than a catalyst. Further investigations are under progress to unveil how cobalt boride catalyzes the hydrogenation reaction of $\text{Li}_2\text{B}_{12}\text{H}_{12-x}$ and to improve the completeness of the reformation of LiBH_4 .

5. Conclusions

We demonstrate the improved rehydrogenation of H-deficient $\text{Li}_2\text{B}_{12}\text{H}_{12-x}$ to reform LiBH_4 . In presence of nanocrystalline cobalt boride, reformation of LiBH_4 from $\text{Li}_2\text{B}_{12}\text{H}_{12-x}$ is achieved under relatively mild conditions (e.g., 400 °C, 100 bar H_2) with a yield of 68%. The active species in the reversible sorption reaction step is suggested to be Co_xB ($x = 1$) based on ^{11}B MAS NMR results. It provides important insights on catalyzing LiBH_4 as a potential reversible hydrogen storage material toward practical applications.

Acknowledgments: We are grateful to the Danish research council (HyNanoBorN). We also like to thank the Swiss National Science Foundation for financial support within the Sinergia project ‘Novel ionic conductors’ under contract number CRSII2_160749/1. The NMR hardware was partially granted by the Swiss National Science Foundation (SNFS, under contract number 206021_150638/1).

Author Contributions: Y.Y., M.Z. and A.R. conceived and designed the experiments; H.W. and W.C. prepared the Co_xB samples, Y.Y. and D.R. performed the experiments and analyzed the data; the paper was written by Y.Y., A.R. and D.R. All authors agreed on the final version of the manuscript.

Conflicts of Interest: The authors declare no conflict of interest.

References

1. Yu, X.; Tang, Z.; Sun, D.; Ouyang, L.; Zhu, M. Recent advances and remaining challenges of nanostructured materials for hydrogen storage applications. *Prog. Mater. Sci.* **2017**, *88*, 1–48. [[CrossRef](#)]
2. Paskevicius, M.; Jepsen, L.H.; Schouwink, P.; Cerny, R.; Ravnsbaek, D.B.; Filinchuk, Y.; Dornheim, M.; Besenbacher, F.; Jensen, T.R. Metal borohydrides and derivatives - synthesis, structure and properties. *Chem. Soc. Rev.* **2017**, *46*, 1565–1634. [[CrossRef](#)] [[PubMed](#)]
3. Moller, K.T.; Jensen, T.R.; Akiba, E.; Li, H.W. Hydrogen—A sustainable energy carrier. *Prog. Nat. Sci.-Mater.* **2017**, *27*, 34–40. [[CrossRef](#)]
4. He, T.; Pachfule, P.; Wu, H.; Xu, Q.; Chen, P. Hydrogen carriers. *Nat. Rev. Mater.* **2016**, *1*, 16059. [[CrossRef](#)]
5. Lai, Q.; Paskevicius, M.; Sheppard, D.A.; Buckley, C.E.; Thornton, A.W.; Hill, M.R.; Gu, Q.; Mao, J.; Huang, Z.; Liu, H.K.; et al. Hydrogen storage materials for mobile and stationary applications: Current state of the art. *ChemSuschem* **2015**, *8*, 2789–2825. [[CrossRef](#)] [[PubMed](#)]
6. Orimo, S.I.; Nakamori, Y.; Eliseo, J.R.; Zuttel, A.; Jensen, C.M. Complex hydrides for hydrogen storage. *Chem. Rev.* **2007**, *107*, 4111–4132. [[CrossRef](#)] [[PubMed](#)]
7. Soulie, J.P.; Renaudin, G.; Cerny, R.; Yvon, K. Lithium boro-hydride LiBH_4 . *J. Alloy Compd.* **2002**, *346*, 200–205. [[CrossRef](#)]

8. Zuttel, A.; Rentsch, S.; Fischer, P.; Wenger, P.; Sudan, P.; Mauron, P.; Emmenegger, C. Hydrogen storage properties of LiBH_4 . *J. Alloy Compd.* **2003**, *356*, 515–520. [[CrossRef](#)]
9. Orimo, S.; Nakamori, Y.; Kitahara, G.; Miwa, K.; Ohba, N.; Towata, S.; Züttel, A. Dehydrogenating and rehydrogenating reactions of LiBH_4 . *J. Alloy Compd.* **2005**, *404*, 427–430. [[CrossRef](#)]
10. Orimo, S.I.; Nakamori, Y.; Ohba, N.; Miwa, K.; Aoki, M.; Towata, S.; Zuttel, A. Experimental studies on intermediate compound of LiBH_4 . *Appl. Phys. Lett.* **2006**, *89*, 021920. [[CrossRef](#)]
11. Mauron, P.; Buchter, F.; Friedrichs, O.; Remhof, A.; Biemann, M.; Zwicky, C.N.; Zuttel, A. Stability and reversibility of LiBH_4 . *J. Phys. Chem. B* **2008**, *112*, 906–910. [[CrossRef](#)] [[PubMed](#)]
12. Her, J.H.; Yousufuddin, M.; Zhou, W.; Jalisatgi, S.S.; Kulleck, J.G.; Zan, J.A.; Hwang, S.J.; Bowman, R.C.; Udovic, T.J. Crystal structure of $\text{Li}_2\text{B}_{12}\text{H}_{12}$: A possible intermediate species in the decomposition of LiBH_4 . *Inorg. Chem.* **2008**, *47*, 9757–9759. [[CrossRef](#)] [[PubMed](#)]
13. Yan, Y.G.; Remhof, A.; Hwang, S.J.; Li, H.W.; Mauron, P.; Orimo, S.; Zuttel, A. Pressure and temperature dependence of the decomposition pathway of LiBH_4 . *Phys. Chem. Chem. Phys.* **2012**, *14*, 6514–6519. [[CrossRef](#)] [[PubMed](#)]
14. Pitt, M.P.; Paskevicius, M.; Brown, D.H.; Sheppard, D.A.; Buckley, C.E. Thermal stability of $\text{Li}_2\text{B}_{12}\text{H}_{12}$ and its role in the decomposition of LiBH_4 . *J. Am. Chem. Soc.* **2013**, *135*, 6930–6941. [[CrossRef](#)] [[PubMed](#)]
15. Cai, W.; Wang, H.; Liu, J.; Jiao, L.; Wang, Y.; Ouyang, L.; Sun, T.; Sun, D.; Wang, H.; Yao, X.; et al. Towards easy reversible dehydrogenation of LiBH_4 by catalyzing hierarchic nanostructured cob. *Nano Energy* **2014**, *10*, 235–244. [[CrossRef](#)]
16. Shao, J.; Xiao, X.Z.; Fan, X.L.; Huang, X.; Zhai, B.; Li, S.Q.; Ge, H.W.; Wang, Q.D.; Chen, L.X. Enhanced hydrogen storage capacity and reversibility of LiBH_4 nanoconfined in the densified zeolite-templated carbon with high mechanical stability. *Nano Energy* **2015**, *15*, 244–255. [[CrossRef](#)]
17. White, J.L.; Newhouse, R.J.; Zhang, J.Z.; Udovic, T.J.; Stavila, V. Understanding and mitigating the effects of stable dodecahydro-closo-dodecaborate intermediates on hydrogen-storage reactions. *J. Phys. Chem. C* **2016**, *120*, 25725–25731. [[CrossRef](#)]
18. Ngene, P.; Verkuijlen, M.H.W.; Barre, C.; Kentgens, A.P.M.; de Jongh, P.E. Reversible Li-insertion in nanoscaffolds: A promising strategy to alter the hydrogen sorption properties of Li-based complex hydrides. *Nano Energy* **2016**, *22*, 169–178. [[CrossRef](#)]
19. Vajo, J.J.; Skeith, S.L.; Mertens, F. Reversible storage of hydrogen in destabilized LiBH_4 . *J. Phys. Chem. B* **2005**, *109*, 3719–3722. [[CrossRef](#)] [[PubMed](#)]
20. Pinkerton, F.E.; Meyer, M.S.; Meisner, G.P.; Balogh, M.P.; Vajo, J.J. Phase boundaries and reversibility of $\text{LiBH}_4/\text{MgH}_2$ hydrogen storage material. *J. Phys. Chem. C* **2007**, *111*, 12881–12885. [[CrossRef](#)]
21. Au, M.; Jurgensen, A.R.; Spencer, W.A.; Anton, D.L.; Pinkerton, F.E.; Hwang, S.J.; Kim, C.; Bowman, R.C. Stability and reversibility of lithium borohydrides doped by metal halides and hydrides. *J. Phys. Chem. C* **2008**, *112*, 18661–18671. [[CrossRef](#)]
22. Blanchard, D.; Shi, Q.; Boothroyd, C.B.; Vegge, T. Reversibility of Al/Ti modified LiBH_4 . *J. Phys. Chem. C* **2009**, *113*, 14059–14066. [[CrossRef](#)]
23. Nielsen, T.K.; Bosenberg, U.; Gosalawit, R.; Dornheim, M.; Cerenius, Y.; Besenbacher, F.; Jensen, T.R. A reversible nanoconfined chemical reaction. *ACS Nano* **2010**, *4*, 3903–3908. [[CrossRef](#)] [[PubMed](#)]
24. Shim, J.H.; Lim, J.H.; Rather, S.U.; Lee, Y.S.; Reed, D.; Kim, Y.; Book, D.; Cho, Y.W. Effect of hydrogen back pressure on dehydrogenation behavior of LiBH_4 -based reactive hydride composites. *J. Phys. Chem. Lett.* **2010**, *1*, 59–63. [[CrossRef](#)]
25. Choi, Y.J.; Lu, J.; Sohn, H.Y.; Fang, Z.Z.; Kim, C.; Bowman, R.C.; Hwang, S.J. Reaction mechanisms in the $\text{Li}_3\text{AlH}_6/\text{LiBH}_4$ and Al/LiBH_4 systems for reversible hydrogen storage. Part 2: Solid-state NMR studies. *J. Phys. Chem. C* **2011**, *115*, 6048–6056. [[CrossRef](#)]
26. Cai, W.T.; Wang, H.; Sun, D.L.; Zhu, M. Nanosize-controlled reversibility for a destabilizing reaction in the $\text{LiBH}_4\text{-NdH}_{2+x}$ system. *J. Phys. Chem. C* **2013**, *117*, 9566–9572. [[CrossRef](#)]
27. Javadian, P.; Sheppard, D.A.; Buckley, C.E.; Jensen, T.R. Hydrogen storage properties of nanoconfined $\text{LiBH}_4\text{-Ca}(\text{BH}_4)_2$. *Nano Energy* **2015**, *11*, 96–103. [[CrossRef](#)]
28. Puzkiel, J.A.; Riglos, M.V.C.; Karimi, F.; Santoru, A.; Pistidda, C.; Klassen, T.; von Colbe, J.M.B.; Dornheim, M. Changing the dehydrogenation pathway of $\text{LiBH}_4\text{-MgH}_2$ via nanosized lithiated TiO_2 . *Phys. Chem. Chem. Phys.* **2017**, *19*, 7455–7460. [[CrossRef](#)] [[PubMed](#)]

29. Kang, X.-D.; Wang, P.; Ma, L.-P.; Cheng, H.-M. Reversible hydrogen storage in LiBH_4 destabilized by milling with al. *Appl. Phys. A* **2007**, *89*, 963–966. [[CrossRef](#)]
30. Song, D.; Wang, Y.; Wang, Y.; Jiao, L.; Yuan, H. Preparation and characterization of novel structure Co–B hydrogen storage alloy. *Electrochem. Commun.* **2008**, *10*, 1486–1489. [[CrossRef](#)]
31. Wang, Q.; Jiao, L.; Du, H.; Song, D.; Peng, W.; Si, Y.; Wang, Y.; Yuan, H. Facile preparation and good electrochemical hydrogen storage properties of chain-like and rod-like Co-B nanomaterials. *Electrochim. Acta* **2010**, *55*, 7199–7203. [[CrossRef](#)]
32. Massiot, D.; Fayon, F.; Capron, M.; King, I.; LeCalve, S.; Alonso, B.; Durand, J.O.; Bujoli, B.; Gan, Z.H.; Hoatson, G. Modelling one- and two-dimensional solid-state nmr spectra. *Magn. Reson. Chem.* **2002**, *40*, 70–76. [[CrossRef](#)]
33. Yan, Y.G.; Remhof, A.; Mauron, P.; Rentsch, D.; Lodziana, Z.; Lee, Y.S.; Lee, H.S.; Cho, Y.W.; Zuttel, A. Controlling the dehydrogenation reaction toward reversibility of the LiBH_4 - $\text{Ca}(\text{BH}_4)_2$ eutectic system. *J. Phys. Chem. C* **2013**, *117*, 8878–8886. [[CrossRef](#)]
34. Bykova, E.; Tsirlin, A.A.; Gou, H.; Dubrovinsky, L.; Dubrovinskaia, N. Novel non-magnetic hard boride Co_5B_{16} synthesized under high pressure. *J. Alloy Compd.* **2014**, *608*, 69–72. [[CrossRef](#)]
35. Chikazumi, S. *Physics of Ferromagnetism*, 2nd ed.; Oxford University Press: Oxford, UK, 1997.
36. Wu, C.; Wu, F.; Bai, Y.; Yi, B.; Zhang, H. Cobalt boride catalysts for hydrogen generation from alkaline NaBH_4 solution. *Mater. Lett.* **2005**, *59*, 1748–1751. [[CrossRef](#)]
37. Tang, W.S.; Wu, G.; Liu, T.; Wee, A.T.S.; Yong, C.K.; Xiong, Z.; Hor, A.T.S.; Chen, P. Cobalt-catalyzed hydrogen desorption from the LiNH_2 - LiBH_4 system. *Dalton Trans.* **2008**, *0*, 2395–2399. [[CrossRef](#)] [[PubMed](#)]
38. Masa, J.; Weide, P.; Peeters, D.; Sinev, I.; Xia, W.; Sun, Z.; Somsen, C.; Muhler, M.; Schuhmann, W. Amorphous cobalt boride (Co_2B) as a highly efficient nonprecious catalyst for electrochemical water splitting: Oxygen and hydrogen evolution. *Adv. Energy Mater.* **2016**, *6*, 15023131. [[CrossRef](#)]
39. Fernandes, R.; Patel, N.; Miotello, A.; Filippi, M. Studies on catalytic behavior of Co–Ni–B in hydrogen production by hydrolysis of NaBH_4 . *J. Mol. Catal. A* **2009**, *298*, 1–6. [[CrossRef](#)]
40. Carencio, S.; Portehault, D.; Boissière, C.; Mézailles, N.; Sanchez, C. Nanoscaled metal borides and phosphides: Recent developments and perspectives. *Chem. Rev.* **2013**, *113*, 7981–8065. [[CrossRef](#)] [[PubMed](#)]



© 2018 by the authors. Licensee MDPI, Basel, Switzerland. This article is an open access article distributed under the terms and conditions of the Creative Commons Attribution (CC BY) license (<http://creativecommons.org/licenses/by/4.0/>).